Manipulating Non-Abelian Anyons in a Chiral Multichannel Kondo Model

Matan Lotem, Eran Sela, and Moshe Goldstein

Phys. Rev. Lett. **129**, 227703 — Published 23 November 2022

DOI: 10.1103/PhysRevLett.129.227703

Manipulating non-abelian anyons in a chiral multi-channel Kondo model

Matan Lotem,* Eran Sela,† and Moshe Goldstein‡
Raymond and Beverly Sackler School of Physics and Astronomy, Tel Aviv University, Tel Aviv 6997801, Israel

Non-abelian anyons are fractional excitations of gapped topological models believed to describe certain topological superconductors or quantum Hall states. Here, we provide the first numerical evidence that they emerge as independent entities also in gapless electronic models. Starting from a multi-impurity multi-channel chiral Kondo model, we introduce a novel mapping to a single-impurity model, amenable to Wilson's numerical renormalization group. We extract its spectral degeneracy structure and fractional entropy, and calculate the F-matrices, which encode the topological information regarding braiding of anyons, directly from impurity spin-spin correlations. Impressive recent advances on realizing multichannel Kondo systems with chiral edges may thus bring anyons into reality sooner than expected.

Introduction.— Non-abelian anyons are exotic (quasi-)particles which obey neither fermionic nor bosonic statistics, and lie at the heart of topological quantum computing [1, 2]. They define an anyonic fusion-space which can only be transversed by their mutual exchange, or braiding, thus providing topological protection for information encoded in this space. An important class of non-abelian anyons are the $\mathrm{SU}(2)_k$ anyons, which are governed by truncated SU(2) fusion rules [3]. Each such anyon (of topological charge $\frac{1}{2}$) carries with it a quantum dimension of $d_k{=}2\cos\left(\frac{\pi}{2+k}\right)$, which gives the degeneracy per anyon in the thermodynamic limit. Prominent examples are the Ising ($k{=}2, d_2{=}\sqrt{2}$) and Fibonacci ($k{=}3, d_3{=}\frac{1+\sqrt{5}}{2}$) anyons, predicted to arise, e.g., in the $\nu{=}\frac{5}{2}$ and $\nu{=}\frac{12}{5}$ fractional quantum Hall states, respectively [4, 5], and Majorana "fermions" (also $k{=}2$), which arise in a variety of topological systems, e.g., pinned to vortices in 2D topological superconductors [6–8] or on the edges of superconducting nano-wires [9, 10]. However, these quasi-particles prove to be extremely elusive, with no clear experimental evidence for their non-abelian nature.

Another system governed by $\mathrm{SU}(2)_k$ fusion rules, although not of topological nature, is the k-channel Kondo effect [11, 12]. This was most clearly demonstrated by Emery and Kivelson [13], who formulated the solution of the two-channel Kondo effect in terms of Majorana operators. Importantly, this effect has already been observed in tunable nano-structures, for both $k{=}2$ [14–18] and $k{=}3$ [19] channels. The Kondo effect occurs when a quantum impurity, e.g., a spin-$\frac{1}{2}$, is coupled antiferromagnetically to (multiple) non-interacting spinfull fermionic bath(s), i.e., channel(s). For a single channel, at temperatures below the Kondo temperature, the fermions in the bath screen the impurity, which can be interpreted as the impurity binding a fermion from the bath and forming a singlet with it. Going to multiple channels, each channel independently contributes a single screening fermion, but this leads to frustration and fractionalization of the impurity degrees of freedom. The fractionalized quasi-particle comes with a zero-temperature entropy of $\log d_k$, corresponding to the quantum dimension of a single $\mathrm{SU}(2)_k$ charge-$\frac{1}{2}$ anyon [20]. Indeed, the low-energy physics of the k-channel spin-$s \leq \frac{k}{2}$ Kondo effect are captured by a conformal field theory (CFT) in which a single $\mathrm{SU}(2)_k$ anyon with charge s is fused onto the primary fields of (k-channel) free fermions [21, 22].

In order to discuss anyonic statistics, or braiding, we require (i) multiple quasi-particles, and (ii) a physically accessible operator which acts on the anyonic fusion-space. The paradigmatic multi-channel Kondo effect assumes a dilute scenario, so that at temperatures above the Fermi-velocity over the inter-impurity separation (v_F/R), each impurity is effectively coupled to a different bath, thus satisfying (i) but breaking (ii), while for lower temperatures, the bath fermions mediate effective RKKY interactions [23–25] between the impurities, thus resolving the frustration and avoiding emergent fractionalized quasi-particles. It was only recently realized that (i) and (ii) might be reconciled, either by gapping out the bath via superconducting pairing [26] or preventing the generation of interactions in the first place by employing chiral channels [27]. In the latter, fermions (of all channel and spin species) can propagate only in one direction, as on the edge of an integer quantum Hall system, thus preventing backscattering and interference, the mechanisms behind effective interactions. Intuitively, the first impurity encountered by chiral fermions is unaware of the impurities to follow, thus fractionalizing as in the single-impurity case. Repeating this argument sequentially suggests a fractionalized quasi-particle for each impurity. Lopes *et al.* [27] introduced a multiple-impurity extension of the single-impurity multi-channel Kondo CFT fusion as an ansatz for the low-energy behavior of such a system: for each spin-$\frac{1}{2}$ impurity introduce an $\mathrm{SU}(2)_k$ anyon with "topological" charge $\frac{1}{2}$, fuse these anyons to each other, defining a non-abelian fusion space, and then fuse the result onto the free-fermionic primary fields (see examples in Sec. I of [28]). In this ansatz, different fusion outcomes (corresponding to different states in the fusion-space) leave signatures, e.g., on the spatial fermionic correlation functions, which (in principle) can be measured

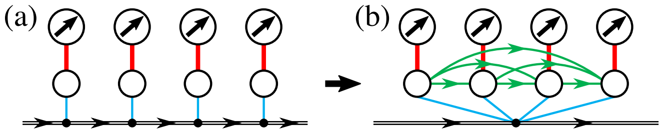

FIG. 1. (a) The impurities are Kondo-coupled to "buffer" dangling sites, which in turn quadratically couple to the chiral channels, and are considered part of the non-interacting bath. (b) Taking the distance between these sites to zero leads to an effective chiral model, in which the dangling sites together with the impurities form a large effective impurity.

by interferometry, enabling measurement-only braiding [29] of quasi-particles. However, in the CFT ansatz the anyons were put in by hand.

In this work we independently test this conjecture, employing a controlled, non-perturbative, numerically exact method – Wilson's numerical renormalization group (NRG) [30], which enables zooming in on the low-energy physics of quantum impurity problems. A key part of NRG is mapping the bath onto a tight-binding (Wilson) chain, but this is incompatible with chirality, as any notion of direction in a (nearest-neighbor) tight-binding chain can be absorbed by gauge transformations. However, chirality is also the solution to the problem. As the distance between the impurities typically enters through interference effects, which are now forbidden, we argue that it does not affect universal properties. This is supported by the results in Ref. [31], in which we numerically account for the distance, as well as by the Bethe-ansatz solution for the Kondo problem [32]. We have the freedom to take the distance between the impurities to be arbitrarily small, as long as we retain the notion of chirality and the ordering of the impurities. We do this by first introducing "buffer sites" between the impurities and the bulk chiral channels, and only then taking the inter-impurity distance to zero. This results in a large effective impurity coupled to a trivial bath, which can readily be plugged into NRG. We then numerically demonstrate that the low-energy behavior of the system indeed corresponds to an $SU(2)_k$ charge-$\frac{1}{2}$ anyon for each impurity, and that the fusion outcome of pairs of such anyons can be probed by measuring inter-impurity spin correlations.

Model and Method.— We start with M spin-$\frac{1}{2}$ impurities with spin operator $\mathbf{S}_m$ where $m \in \{1, ..., M\}$, and a bath of right-moving free fermions

$$H_{\text{chiral}} = \sum_{\alpha\sigma} \int dx \psi^{\dagger}_{\alpha\sigma}(x)\left(-iv_F\partial_x\right)\psi_{\alpha\sigma}(x), \quad (1)$$

with Fermi velocity v_F, spin $\sigma \in \{\uparrow,\downarrow\}$ and channel $\alpha \in \{1, .., k\}$. One can directly couple the impurities to the bath at locations $\{R_m\}$, by writing the Hamiltonian $\sum_m J\mathbf{S}_m \cdot \mathbf{s}(R_m) + H_{\text{chiral}}$, with $J > 0$ the Kondo-coupling and $\mathbf{s}(x) \equiv \sum_{\alpha\sigma} \psi^{\dagger}_{\alpha\sigma}(x)\boldsymbol{\sigma}_{\sigma\sigma'}\psi_{\alpha\sigma'}(x)$ the bath spin at location x. We treat such a model in Ref. [31], by introducing M coupled effective k-channel baths, but this comes with a very high computational price tag, due to the exponential scaling of NRG with the number of channels. Instead, here we employ a mapping which captures the chirality with a single k-channel bath. We first separate the impurities from the bath, as illustrated in Fig. 1(a), by introducing buffer "dangling" fermionic sites coupled to the bath at locations $\{R_m\}$, and then couple the impurities to these dangling sites, arriving at

$$H_{\text{total}} = J\sum_m \mathbf{S}_m \cdot \mathbf{s}_m + H_{\text{dang}} + H_{\text{chiral}}, \quad (2)$$

$$H_{\text{dang}} = \tilde{t}_0 \sum_{m\alpha\sigma}\left(d^{\dagger}_{m\alpha\sigma}\psi_{\alpha\sigma}(R_m) + \psi^{\dagger}_{\alpha\sigma}(R_m)d_{m\alpha\sigma}\right), \quad (3)$$

where $d_{m\alpha\sigma}$ and $\mathbf{s}_m \equiv \sum_{\alpha\sigma} d^{\dagger}_{m\alpha\sigma}\boldsymbol{\sigma}_{\sigma\sigma'}d_{m\alpha\sigma'}$ are the dangling-sites fermionic and spin operators, respectively, $J > 0$ is the Kondo-coupling, and $\tilde{t}_0$ together with the Fermi velocity define a soft cutoff $\Gamma \equiv \frac{\tilde{t}_0^2}{2v_F}$.

Initially we treat the dangling sites together with the chiral channels as the non-interacting bath to which the impurities are coupled. As typical of Kondo problems, the bath dependence of impurity quantities enters (to all orders in the Kondo-coupling J) only through the (retarded) Green function of the bath at the sites coupled to the impurities, i.e., the dangling sites, when these are decoupled from the impurities:

$$\mathbf{g}^R_{\text{dang}}(\omega) = \left(\omega\mathbb{1} - \mathbf{h} - \mathbf{\Sigma}^R(\omega)\right)^{-1}, \quad (4)$$

with $\mathbb{1}$ the $M\times M$ identity matrix, $\mathbf{h}$=0 the single-particle Hamiltonian acting on the dangling sites, and

$$\mathbf{\Sigma}^R_{mm'}(\omega) = -2i\Gamma\Theta\left(R_{m'} - R_m\right)e^{i\omega(R_{m'}-R_m)/v_F}, \quad (5)$$

the retarded self-energy due to the coupling of the dangling sites to the chiral channels, where $\Theta(x)$ is the Heaviside step function (taking $\Theta(0) = \frac{1}{2}$). A clear signature of chirality (assuming right-movers) is that any retarded quantity at location r due to an event at $r' > r$ vanishes. And indeed, all elements below the diagonal of $\mathbf{\Sigma}^R(\omega)$ are zero, as a result of which the same holds for $\mathbf{g}^R_{\text{dang}}(\omega)$. Thus the introduction of the dangling sites importantly retains chirality. The obtained model is formally equivalent to one without dangling sites in the $\Gamma \to \infty$ limit, whereas for finite Γ we have merely modified the bath density of states to a Lorentzian of width Γ at each dangling site, which should not affect the universal low-energy properties. Assuming $J < \Gamma$, we can define the Kondo temperature as $T_K = \Gamma e^{-\pi\Gamma/J}$.

We now take the limit $\omega(R_M - R_1)/v_F \to 0$, corresponding to low temperatures or long wave-lengths. This limit is taken after the infinite bandwidth limit of Eq. (1), and is not impaired by the soft cutoff Γ. $\mathbf{\Sigma}^R(\omega)$ looses its frequency dependence, but not its chirality, and can be written as

$$\mathbf{\Sigma}^R_{mm'} \to -i\Gamma\begin{cases} 2 & m'>m \\ 1 & m'=m \\ 0 & m'<m \end{cases} \equiv \mathbf{h}^{\text{eff}}_{mm'} - i\Gamma, \quad (6)$$

with $\mathbf{h}^{\text{eff}}$ an Hermitian matrix. Thus $\mathbf{h}^{\text{eff}}$ can be interpreted as an effective (single-particle) Hamiltonian coupling all dangling sites to each other via imaginary hopping amplitudes, while $-i\Gamma$ describes a single trivial bath coupled equally to all dangling sites, i.e.,

$$H_{\text{dang}}^{\text{eff}} = \sum_{\alpha\sigma} \sum_{m>m'} it'_{mm'} \left(d^{\dagger}_{m\alpha\sigma} d_{m'\alpha\sigma} - d^{\dagger}_{m'\alpha\sigma} d_{m\alpha\sigma} \right) + \sqrt{M}\tilde{t}_0 \sum_{m\alpha\sigma} \left(d^{\dagger}_{m\alpha\sigma} \psi_{\alpha\sigma}(0) + \psi^{\dagger}_{\alpha\sigma}(0) d_{m\alpha\sigma} \right), \quad (7)$$

with $t'_{mm'} = \Gamma$. Replacing H_{dang} in Eq. (2) with $H_{\text{dang}}^{\text{eff}}$, we arrive at the model depicted in Fig. 1(b).

Let us review what we have achieved. The obtained model is still chiral (for the very specific choice of $t'_{mm'}$), and reproduces the bath Green function in the low temperature limit. But now we can interpret the impurities together with the dangling sites as a large effective impurity, coupled to an effective bath (described only by H_{chiral}) at a single location, so that its chirality is no longer important. The resulting structure also hints at first fusing all the impurities together, and then fusing onto a single (multi-channel) bath, as in the CFT ansatz of Ref. [27]. The obtained model is amendable to standard NRG, although one still needs to account for the multiple channels. In order to reduce the computational cost, we exploit the different symmetries of the model (charge, spin, channel), using the QSPACE tensor network library, which treats abelian and non-abelian symmetries on equal footing [33–35]. For implementation details see Sec. III in [28] and Refs. [36–39] therein. In order to apply NRG, we introduce an artificial sharp high-energy cutoff $D \gg \Gamma, J$ to the bath density of states. This cutoff, and to a lesser extent the NRG discretization and truncation, mimic the effect of the bulk bands (Landau levels), setting a finite bandwidth for the chiral mode, and mediating effective non-chiral RKKY interactions between the impurities. The latter are expected to decay exponentially with both the bulk gap and the inter-impurity distance [40–42], and are thus eliminated by numerically tuning each $t'_{mm'}$ slightly away from Γ to re-instate chirality (see Sec. IV D in [28]).

Results.— We apply NRG to the effective Hamiltonian for 2 channels with up to 3 impurities, and for 3 channels with up to 2 impurities. In Fig. 2 we plot the impurity entropy S_{imp}, defined as the difference between the entropy of the full system and that of the fermionic bath (dangling sites + chiral channels) in the absence of the impurities, which quantifies the effective degree of freedom d_{eff} each impurity introduces. We find that d_{eff} is independent of the number of impurities M, so that $S_{\text{imp}}/M = \log d_{\text{eff}}(k,T)$ follows the universal single-impurity curve, matching the limit of infinitely separated impurities, and thus supporting our argument that in a chiral system the inter-impurity distance is not important. At high temperatures each impurity is effectively a free spin, contributing a $d_{\text{eff}}{=}2$ degree of freedom. Going below the Kondo temperature while assuming the thermodynamic limit for the bath, each impurity contributes a fractional degree of freedom $d_{\text{eff}}{=}d_k$ corresponding exactly to an $\text{SU}(2)_k$ anyon. These results are well known in the single-impurity scenario [20], but the scaling to multiple impurities, implying an anyon for each impurity, is quite remarkable. This is very different from the paradigmatic multi-impurity multi-channel scenario, where the initially similar entropy curves break for temperatures below $\sim v_F/R$ due to coherent backscattering which generates effective RKKY interaction. In order to probe anyonic statistics we need coherence, and indeed in our case we are already in the regime of $T \ll v_F/R \to \infty$, but now due to chirality, backscattering is forbidden, and the anyons survive.

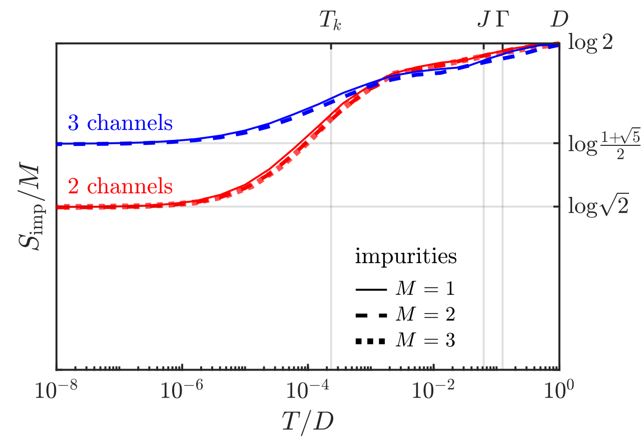

FIG. 2. Impurity entropy per impurity for 2 channels (red) with 1-3 impurities, and 3 channels (blue) with 1,2 impurities, taking $2J{=}\Gamma{=}D/8$. At high temperatures the impurity spins are free, each contributing an entropy of $\log 2$. At low temperatures each impurity contributes a fractional entropy corresponding to the quantum dimension of Ising $(\text{SU}(2)_2)$ or Fibonacci $(\text{SU}(2)_3)$ anyons for 2 or 3 channels, respectively.

The curves in Fig. 2 were obtained for the specific choice of the dangling-sites hopping amplitudes $t'_{mm'}$ which renders the system chiral. We can characterize this point by artificially tuning away from it, and demonstrate that at the chiral point, the low-energy theory is exactly that of the CFT ansatz of Ref. [27]. This is best observed in the finite-size spectrum obtained by NRG, but as its analysis is quite technical, we defer it to Sec. II in [28]. Instead, here we discuss more intuitive quantities.

For two impurities, with either 2 or 3 channels, we find that the effective system undergoes a quantum phase transition from a Kondo-screened spin-1 impurity when the single parameter t'_{12} is below some critical value to a spin-0 “Kondo” effect above it, similar to the two-impurity Kondo-RKKY phase transition [43]. The two phases can be identified by their low-energy spectra (see Sec. II in [28]), with the transition observed, e.g., in the inter-impurity spin-correlator $\langle \mathbf{S}_1 \cdot \mathbf{S}_2 \rangle_{T\to 0}$, which flips sign from positive (triplet-like) to negative (singlet-like), as shown in Fig. 3(a). Tuning away from criticality and projecting the operator $\mathbf{S}_1 \cdot \mathbf{S}_2$ down to the low-energy subspace, we find it is a constant (equal to $\langle \mathbf{S}_1 \cdot \mathbf{S}_2 \rangle_{T\to 0}$), and thus commutes with the low-energy Hamiltonian. This is consistent with our characterization of the two phases, but is not trivial, as $\mathbf{S}_1 {\cdot} \mathbf{S}_2$ does not commute with the full Hamiltonian, and hence the definite spin states (singlet and triplet) mix low- and high-energy states. The critical t'_{12} is exactly the hopping amplitude required for the system to be chiral (it indeed converges to Γ for $D \gg \Gamma, J$, see Fig. S4(a) in [28]). The projected $\mathbf{S}_1 \cdot \mathbf{S}_2$ also commutes with the low-energy Hamiltonian at this point, but now has two eigenvalues, positive and negative. Projecting onto the subspace corresponding to the negative (positive) eigenvalue takes us back to the spin-0 (spin-1) Kondo phase. Thus, at the chiral point, the low-energy Hamiltonian is the direct sum of the low-energy Hamiltonians of the spin-0 and spin-1 Kondo effects. Remembering these can be obtained by fusing an $\mathrm{SU}(2)_k$ charge-0 or 1 anyon to the k-channel bath, we see that in the chiral case we fuse two charge-$\frac{1}{2}$ anyons to the bath

$$0 \times \mathrm{Bath} + 1 \times \mathrm{Bath} = (0+1) \times \mathrm{Bath} = \tfrac{1}{2} \times \tfrac{1}{2} \times \mathrm{Bath},$$

in perfect agreement with the CFT ansatz of Ref. [27]. As a byproduct we have also demonstrated that a (low-energy) measurement of the spin-correlator $\mathbf{S}_1 \cdot \mathbf{S}_2$ actually measures the fusion outcome of the two anyons. We note that this relation between the fusion channel and the spin-correlator was also recently demonstrated analytically in the limits of $k{=}2$ and large-k channels [44].

This suggests we can extract the anyonic F-matrix, which fully characterizes the non-abelian part of the anyonic theory [3], from measurements of different pairwise spin-correlators, as depicted in Fig. 3(b). We explicitly demonstrate this for 3 impurities and 2 channels. We now tune two parameters: the nearest-neighbor $t'_{12} = t'_{23}$ (equal by symmetry) and next-nearest-neighbor t'_{13} hopping amplitudes. For general values the effective low-energy Hamiltonian is that of a single spin-$\frac{1}{2}$ two-channel Kondo (2CK) effect, H_{2CK}. However, at a single critical point, corresponding to the system being chiral, we get a two-fold degeneracy (for each energy eigenstate) on-top of this 2CK effect. We can thus write the low-energy Hamiltonian as a direct sum of two 2CK low-energy Hamiltonians $H_{2CK} {\oplus} H_{2CK}$, each given by CFT by fusing a charge-$\frac{1}{2}$ anyon to the bath

$$\left(\tfrac{1}{2} + \tfrac{1}{2}\right) \times \mathrm{Bath} = (0+1) \times \tfrac{1}{2} \times \mathrm{Bath} = \tfrac{1}{2} \times \tfrac{1}{2} \times \tfrac{1}{2} \times \mathrm{Bath}.$$

This is equivalent to fusing three charge-$\frac{1}{2}$ anyons to the bath, again in perfect agreement with the CFT ansatz of Ref. [27]. We see that the degeneracy is associated to a decoupled fusion-space, and can write the low-energy Hamiltonian as an outer product $H_{2CK} {\otimes} \mathbb{1}_{2\times 2}$, acting on the "energy space" and (trivially) on the fusion space.

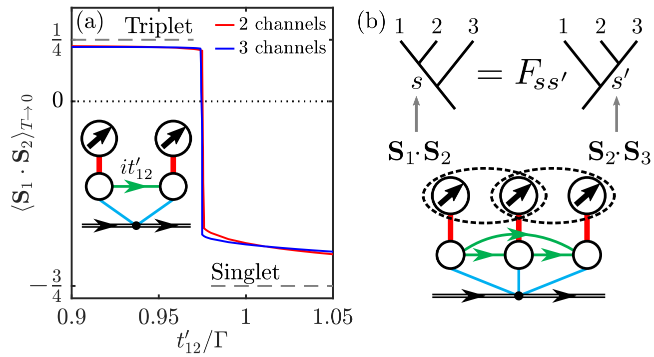

FIG. 3. (a) Quantum phase transition for two impurities with 2 (red) and 3 (blue) channels as a function of the dangling-sites hopping amplitude t'_{12}, taking $2J{=}\Gamma{=}D/8$. Correlations for a bare singlet / triplet are indicated by dashed lines. (b) Extraction of the F-matrix from inter-impurity spin correlators in a three-impurity system.

Projecting the three pairwise spin-correlators $\mathbf{S}_1 {\cdot}\, \mathbf{S}_2$, $\mathbf{S}_2 {\cdot}\, \mathbf{S}_3$, and $\mathbf{S}_1 {\cdot}\, \mathbf{S}_3$ down to the low-energy subspace, we find all three commute with the low-energy Hamiltonian, and act non-trivially only on the fusion-space. Thus, for each pair of impurities m, m' the projected $\mathbf{S}_m {\cdot}\, \mathbf{S}_{m'}$ can be written as $\mathbb{1}_{2CK} \otimes \mathbf{s}_{mm'}$, where $\mathbb{1}_{2CK}$ is the identity matrix in the "energy space" and $\mathbf{s}_{mm'}$ is a $2{\times}2$ Hermitian matrix. Diagonalizing $\mathbf{s}_{mm'}$ we find that it (and thus $\mathbf{S}_m {\cdot}\, \mathbf{S}_{m'}$) has one negative (singlet-like) and one positive (triplet-like) eigenvalue, with eigenstates $|0_{mm'}\rangle$ and $|1_{mm'}\rangle$, respectively. The different correlators do not commute with each other, and so define different bases for the fusion space, related by the basis transformation

$$F = \begin{pmatrix} \langle 0_{12} \,|\, 0_{23} \rangle & \langle 0_{12} \,|\, 1_{23} \rangle \\ \langle 1_{12} \,|\, 0_{23} \rangle & \langle 1_{12} \,|\, 1_{23} \rangle \end{pmatrix} = \frac{1}{\sqrt{2}} \begin{pmatrix} 1.003 & 0.997 \\ 0.997 & -1.003 \end{pmatrix}. \quad (8)$$

For concreteness we have restricted ourselves to the relation between the eigenbases of $\mathbf{S}_1 {\cdot}\, \mathbf{S}_2$ and $\mathbf{S}_2 {\cdot}\, \mathbf{S}_3$, and presented the numerically extracted values in this case. We note that this result displays dependence on the ratio J/Γ, which we discuss in Sec. IV of [28]. Interpreting the eigenstates of the spin-correlator $\mathbf{S}_m {\cdot}\, \mathbf{S}_{m'}$ as states with definite fusion outcomes of anyons m and m' (as in the two-impurity case), Eq. (8) exactly defines the F-matrix, which matches $\frac{1}{\sqrt{2}} \left(\begin{smallmatrix} 1 & 1 \\ 1 & -1 \end{smallmatrix} \right)$ corresponding to $\mathrm{SU}(2)_2$ anyons.

Conclusions.— We have numerically demonstrated that multiple Kondo impurities coupled to k chiral channels (i) host multiple $\mathrm{SU}(2)_k$ non-abelian anyons (one per impurity), highlighted by the fractional entropy contribution per impurity, and (ii) the emergence of a decoupled fusion-space, which can be probed by low-energy measurements of the inter-impurity spin-correlators, explicitly extracting the F-matrix of $\mathrm{SU}(2)_2$ anyons. We can now braid the anyons by a measurement-only protocol [29], which teleports them using only measurements of pairwise topological charge (fusion channel). One can envision implementing this protocol, e.g., by a low-energy scattering experiment, directly demonstrating the non-abelian nature of the anyons in the system.

Experiments consisting of a single impurity coupled to 2 and 3 integer quantum Hall edge-states (i.e., chiral channels) have already been carried out [18, 19], with clear signatures of the fractionalized degrees of freedom [45–48]. Extending these experiments to multiple impurities with all spin and channel species propagating between the impurities is a challenge. Testing if more realistic setups, in which only some of the species connect the impurities while the remainder are local to each impurity, also support non-abelian anyons, and what physical observables probe their fusion-space is quite straightforward for the method presented, and is left for future work. Note that due the absence of a (topological) gap, we expect information encoded in the fusion space to decohere as a power law of T/T_K, in contrast to the exponential suppression in the presence of a gap. Still, based on the success of [18, 19], the path to observing non-abelian anyons might be shorter in these systems.

Acknowledgments.— We would like to thank J. von Delft, A. Weichselbaum and S.-S. Lee for fruitful discussions, as well as sharing the QSpace tensor-network library and accompanying code [33–35, 49]. E.S. was supported by the Synergy funding for Project No. 941541, ARO (W911NF-20-1-0013), the US-Israel Binational Science Foundation (BSF) Grant No. 2016255, and the Israel Science Foundation (ISF) Grant No. 154/19. M.G. was supported by the ISF and the Directorate for Defense Research and Development (DDR&D) Grant No. 3427/21 and by the BSF Grant No. 2020072.

* matanlotem@mail.tau.ac.il
† eransx@googlemail.com
‡ mgoldstein@tauex.tau.ac.il

[1] A. Y. Kitaev, Fault-tolerant quantum computation by anyons, Annals of Physics **303**, 2 (2003).
[2] C. Nayak, S. H. Simon, A. Stern, M. Freedman, and S. Das Sarma, Non-Abelian anyons and topological quantum computation, Reviews of Modern Physics **80**, 1083 (2008).
[3] P. H. Bonderson, *Non-Abelian Anyons and Interferometry*, Ph.D. thesis, California Institute of Technology (2007).
[4] G. Moore and N. Read, Nonabelions in the fractional quantum hall effect, Nuclear Physics B **360**, 362 (1991).
[5] N. Read and E. Rezayi, Beyond paired quantum Hall states: Parafermions and incompressible states in the first excited Landau level, Physical Review B **59**, 8084 (1999).
[6] N. Read and D. Green, Paired states of fermions in two dimensions with breaking of parity and time-reversal symmetries and the fractional quantum Hall effect, Physical Review B **61**, 10267 (2000).
[7] D. A. Ivanov, Non-Abelian Statistics of Half-Quantum Vortices in p-Wave Superconductors, Physical Review Letters **86**, 268 (2001).
[8] L. Fu and C. L. Kane, Superconducting Proximity Effect and Majorana Fermions at the Surface of a Topological Insulator, Physical Review Letters **100**, 096407 (2008).
[9] R. M. Lutchyn, J. D. Sau, and S. Das Sarma, Majorana Fermions and a Topological Phase Transition in Semiconductor-Superconductor Heterostructures, Physical Review Letters **105**, 077001 (2010).
[10] Y. Oreg, G. Refael, and F. von Oppen, Helical Liquids and Majorana Bound States in Quantum Wires, Physical Review Letters **105**, 177002 (2010).
[11] P. Nozières and A. Blandin, Kondo effect in real metals, Journal de Physique **41**, 193 (1980).
[12] A. C. Hewson, *The Kondo Problem to Heavy Fermions*, Cambridge Studies in Magnetism (Cambridge University Press, Cambridge, 1993).
[13] V. J. Emery and S. Kivelson, Mapping of the two-channel Kondo problem to a resonant-level model, Physical Review B **46**, 10812 (1992).
[14] R. M. Potok, I. G. Rau, H. Shtrikman, Y. Oreg, and D. Goldhaber-Gordon, Observation of the two-channel Kondo effect, Nature **446**, 167 (2007).
[15] H. T. Mebrahtu, I. V. Borzenets, D. E. Liu, H. Zheng, Y. V. Bomze, A. I. Smirnov, H. U. Baranger, and G. Finkelstein, Quantum phase transition in a resonant level coupled to interacting leads, Nature **488**, 61 (2012).
[16] H. T. Mebrahtu, I. V. Borzenets, H. Zheng, Y. V. Bomze, A. I. Smirnov, S. Florens, H. U. Baranger, and G. Finkelstein, Observation of Majorana quantum critical behaviour in a resonant level coupled to a dissipative environment, Nature Physics **9**, 732 (2013).
[17] A. J. Keller, L. Peeters, C. P. Moca, I. Weymann, D. Mahalu, V. Umansky, G. Zaránd, and D. Goldhaber-Gordon, Universal Fermi liquid crossover and quantum criticality in a mesoscopic system, Nature **526**, 237 (2015).
[18] Z. Iftikhar, S. Jezouin, A. Anthore, U. Gennser, F. D. Parmentier, A. Cavanna, and F. Pierre, Two-channel Kondo effect and renormalization flow with macroscopic quantum charge states, Nature **526**, 233 (2015).
[19] Z. Iftikhar, A. Anthore, A. K. Mitchell, F. D. Parmentier, U. Gennser, A. Ouerghi, A. Cavanna, C. Mora, P. Simon, and F. Pierre, Tunable quantum criticality and super-ballistic transport in a "charge" Kondo circuit, Science **360**, 1315 (2018).
[20] A. M. Tsvelick, The thermodynamics of multichannel Kondo problem, Journal of Physics C: Solid State Physics **18**, 159 (1985).
[21] I. Affleck and A. W. W. Ludwig, The Kondo effect, conformal field theory and fusion rules, Nuclear Physics B **352**, 849 (1991).
[22] I. Affleck and A. W. W. Ludwig, Critical theory of overscreened Kondo fixed points, Nuclear Physics B **360**, 641 (1991).
[23] M. A. Ruderman and C. Kittel, Indirect Exchange Coupling of Nuclear Magnetic Moments by Conduction Electrons, Physical Review **96**, 99 (1954).
[24] T. Kasuya, A Theory of Metallic Ferro- and Antiferromagnetism on Zener's Model, Progress of Theoretical Physics **16**, 45 (1956).
[25] K. Yosida, Magnetic Properties of Cu-Mn Alloys, Physical Review **106**, 893 (1957).
[26] Y. Komijani, Isolating Kondo anyons for topological quantum computation, Physical Review B **101**, 235131

(2020).
[27] P. L. S. Lopes, I. Affleck, and E. Sela, Anyons in multichannel Kondo systems, Physical Review B **101**, 085141 (2020).
[28] See Supplemental Material.
[29] P. Bonderson, M. Freedman, and C. Nayak, Measurement-Only Topological Quantum Computation, Physical Review Letters **101**, 010501 (2008).
[30] K. G. Wilson, The renormalization group: Critical phenomena and the Kondo problem, Reviews of Modern Physics **47**, 773 (1975).
[31] M. Lotem, E. Sela, and M. Goldstein, The Chiral Numerical Renormalization Group (2022), arXiv:2208.02283 [cond-mat].
[32] N. Andrei, K. Furuya, and J. H. Lowenstein, Solution of the Kondo problem, Reviews of Modern Physics **55**, 331 (1983).
[33] A. Weichselbaum, Tensor networks and the numerical renormalization group, Physical Review B **86**, 245124 (2012).
[34] A. Weichselbaum, Non-abelian symmetries in tensor networks: A quantum symmetry space approach, Annals of Physics **327**, 2972 (2012).
[35] A. Weichselbaum, X-symbols for non-Abelian symmetries in tensor networks, Physical Review Research **2**, 023385 (2020).
[36] R. Bulla, T. A. Costi, and T. Pruschke, Numerical renormalization group method for quantum impurity systems, Reviews of Modern Physics **80**, 395 (2008).
[37] V. L. Campo and L. N. Oliveira, Alternative discretization in the numerical renormalization-group method, Physical Review B **72**, 104432 (2005).
[38] R. Žitko, Adaptive logarithmic discretization for numerical renormalization group methods, Computer Physics Communications **180**, 1271 (2009).
[39] J. J. Sakurai and J. Napolitano, *Modern Quantum Mechanics*, 2nd ed. (Cambridge University Press, Cambridge, 2017).
[40] N. Bloembergen and T. J. Rowland, Nuclear Spin Exchange in Solids: Tl^{203} and Tl^{205} Magnetic Resonance in Thallium and Thallic Oxide, Physical Review **97**, 1679 (1955).
[41] P. D. Kurilovich, V. D. Kurilovich, and I. S. Burmistrov, Indirect exchange interaction between magnetic impurities in the two-dimensional topological insulator based on CdTe/HgTe/CdTe quantum wells, Physical Review B **94**, 155408 (2016).
[42] V. D. Kurilovich, P. D. Kurilovich, and I. S. Burmistrov, Indirect exchange interaction between magnetic impurities near the helical edge, Physical Review B **95**, 115430 (2017).
[43] C. Jayaprakash, H. R. Krishna-murthy, and J. W. Wilkins, Two-Impurity Kondo Problem, Physical Review Letters **47**, 737 (1981).
[44] D. Gabay, C. Han, P. L. S. Lopes, I. Affleck, and E. Sela, Multi-impurity chiral Kondo model: Correlation functions and anyon fusion rules, Physical Review B **105**, 035151 (2022).
[45] L. A. Landau, E. Cornfeld, and E. Sela, Charge Fractionalization in the Two-Channel Kondo Effect, Physical Review Letters **120**, 186801 (2018).
[46] G. A. R. van Dalum, A. K. Mitchell, and L. Fritz, Wiedemann-Franz law in a non-Fermi liquid and Majorana central charge: Thermoelectric transport in a two-channel Kondo system, Physical Review B **102**, 041111 (2020).
[47] T. K. T. Nguyen and M. N. Kiselev, Thermoelectric Transport in a Three-Channel Charge Kondo Circuit, Physical Review Letters **125**, 026801 (2020).
[48] C. Han, Z. Iftikhar, Y. Kleeorin, A. Anthore, F. Pierre, Y. Meir, A. K. Mitchell, and E. Sela, Fractional Entropy of Multichannel Kondo Systems from Conductance-Charge Relations, Physical Review Letters **128**, 146803 (2022).
[49] S.-S. B. Lee and A. Weichselbaum, Adaptive broadening to improve spectral resolution in the numerical renormalization group, Physical Review B **94**, 235127 (2016).